

DEVELOPMENT AND EVALUATION OF ACECLOFENAC-LOADED NANOSPONGE HYDROGEL FOR ENHANCED TOPICAL ANTI-INFLAMMATORY DELIVERY

MAYS HASSAN¹, LUBNA A. SABRI^{2*}¹Ministry of Health and Environment, Baghdad Health Directorate, Baghdad, Iraq. ²Department of Pharmaceutics, College of Pharmacy, University of Baghdad*Corresponding author: Lubna A. Sabri; *Email: lobna.sabri@copharm.uobaghdad.edu.iq

Received: 23 Oct 2024, Revised and Accepted: 18 Dec 2024

ABSTRACT

Objective: Aceclofenac (ACE) is a derivative of phenylacetic acid and a non-steroidal anti-inflammatory drug (NSAID) known for its anti-inflammatory, analgesic, and antipyretic properties. This study aims to enhance ACE's solubility and therapeutic efficacy by developing NanoSponges (NS) loaded into a hydrogel for topical drug delivery, addressing the limitations of current ACE formulations, such as rapid metabolism and short half-life.

Methods: NS were synthesized using the emulsion solvent diffusion technique with varying concentrations of Ethyl Cellulose (EC) and Poly Vinyl Alcohol (PVA). Ten NS formulations were evaluated for particle size (PS), Particle Dispersion Index (PDI), Production Yield percentage (PY%), and Entrapment Efficiency percentage (EE%). Fourier Transform Infrared Spectroscopy (FTIR) and Differential Scanning Calorimetry (DSC) analyses confirmed the compatibility between ACE and the excipients. The surface morphology of the NS was examined using Field Emission Scanning Electron Microscopy (FESEM). The optimal Formulation (F2) was integrated into seven hydrogel formulations based on Hydroxy Propyl Methyl Cellulose (HPMC).

Results: The F2 had a PY% of 77.92±2.2%, an EE% of 90.05±1.1%, a PS of 127.3±3.2 nm, and a PDI of 0.1±0.02. The optimal hydrogel formulation (G1) showed a pH of 6.2±0.15, a Drug Content (DC%) of 95.19±0.23%, a spreadability of 9.5±0.2 cm, and a permeation rate of 55.94±1.4% over 8 h. Additionally, G1 demonstrated *in vivo* anti-inflammatory activity of 65.38±1.1% over 24 h and a cumulative drug release of 84.5±3.8% over the same period.

Conclusion: The NS-loaded hydrogel presents a promising strategy for enhancing ACE's therapeutic potential by providing extended drug release and improved stability, effectively addressing the limitations of existing formulations.

Keywords: NS, Hydrogel, *In vitro* permeation study, *In vivo* anti-inflammatory study

© 2025 The Authors. Published by Innovare Academic Sciences Pvt Ltd. This is an open access article under the CC BY license (<https://creativecommons.org/licenses/by/4.0/>) DOI: <https://dx.doi.org/10.22159/ijap.2025v17i2.53014> Journal homepage: <https://innovareacademics.in/journals/index.php/ijap>

INTRODUCTION

The immune system mistakenly assaults healthy cells in the body, leading to inflammation (painful swelling) in the affected areas of the body, making rheumatoid arthritis, an autoimmune and inflammatory disorder. In most cases, rheumatoid arthritis affects numerous joints simultaneously. Symptoms of rheumatoid arthritis include joint involvement in the hands, wrists, and knees. Rheumatoid arthritis attacks a joint by inducing inflammation of the joint lining, destroying the joint tissue. Degeneration of this tissue can result in persistent or chronic discomfort, distortion, and instability. Rheumatoid arthritis has the potential to impact various tissues in the body, leading to pathological conditions in vital organs including the lungs, heart, and eyes [1]. Nanosponge (NS) are a novel category of materials characterized by their small mesh-like NS structures composed of Nanosized particles. These structures have cavity widths of a few nanometers, allowing for the encapsulation of a wide range of substances [2]. The exceptional flexibility of NS is attributed to their ability to encapsulate both hydrophilic and hydrophobic medicinal molecules, facilitated by their features such as inner hydrophobic chambers and exterior hydrophilic branches, therefore enhancing the solubility of molecules with low water solubility [3]. The manufacture of NS depends on the particular delivery mechanism, polymers, and properties of the formulation and solvents. A notable approach utilized for NS development is the Emulsion Solvent Diffusion method, the emulsion solvent diffusion technique was selected over alternatives like ultrasound-assisted synthesis due to its simplicity, scalability, and ability to produce uniform nanoparticles. This method involves dissolving the drug and polymer in a common solvent, followed by emulsification and solvent evaporation, resulting in the formation of nanoparticles. Ultrasound-assisted synthesis, while effective, can be challenging to scale up and may require specialized equipment. Additionally, the emulsion solvent diffusion technique allows for better control over Particle size (PS) and drug loading [4, 5]. Aceclofenac (ACE) is an

ideal option for sustained-release formulations because of its short biological half-life of approximately 4 h and the necessity for more frequent dosing [6]. It exhibits minimal solubility in water but demonstrates substantial solubility in 96% ethanol. ACE is advised to manage symptoms associated with rheumatoid arthritis, osteoarthritis, and ankylosing spondylitis, in both acute and chronic phases [7]. The NS-loaded hydrogel addresses the limitations of current ACE formulations by significantly improving the stability and efficacy of ACE. The NSs encapsulate ACE molecules, protecting them from rapid metabolism and degradation, which extends the drug's therapeutic effect. The hydrogel matrix provides a sustained and controlled drug release over time, ensuring a steady and prolonged therapeutic impact. This method also enhances the bioavailability of ACE, meaning a higher concentration of the drug reaches the target site more effectively [8]. Additionally, topical delivery of ACE is ideal because it reduces gastrointestinal side effects commonly associated with oral administration of NSAIDs. Oral NSAIDs can cause adverse effects such as gastrointestinal bleeding, ulcers, and perforation. By applying ACE topically, the drug bypasses the gastrointestinal tract, thereby minimizing these risks. Additionally, topical delivery provides targeted therapy directly to the affected area, enhancing the drug's efficacy and reducing systemic exposure [9]. Compared to other advanced topical formulations like liposomes and microsponges, NS hydrogels offer superior drug loading capacity and stability. While liposomes are limited in carrying capacity and prone to chemical and microbial instability, NSs provide a more robust and efficient delivery system. Microsponges, although effective, have larger PSs that can disrupt the system, whereas NSs, with their smaller size, impose less risk and offer better control over drug release [10, 11].

MATERIALS AND METHODS

Material

The following ingredients were obtained from China, Zhengzhou, and Fushi Technology: ACE powder and PVA polymers.

DiChloroMethane (DCM) was acquired from Germany: Merck KGaA. EC was given by Samara Drug Industry, Samara, Iraq. Dialysis bag (MWco 8000-14000 D) was purchased from Special Product Laboratory, USA. Polyethylene glycol 400, Potassium dihydrogen phosphate, Disodium hydrogen phosphate, and sodium chloride were purchased from Loba Chem, India, and a Micro porous membrane of 0.22µm was purchased from ANOW, China. Absolute ethanol 99% was produced by Honeywell in Böblingen, Germany. And HPMC (K100) from Alpha Chemika, India.

Method

Formulation of NSs

The summary of the composition of the synthesized is provided in table 1. The synthesis of ACE NS is achieved by the emulsion solvent

diffusion technique [12]. An ultrasonic shaker (Copley Scientific, UK) was employed to solubilize ACE and EC in 5 ml of DCM, therefore forming the internal phase. The external phase consisted of 50 ml of Distilled Water (D. W.) with dissolved PVA. Using a hot plate magnetic stirrer (Joan lab, China) at different rates of Revolutions Per Minute (RPM), the internal phase was then incrementally introduced to the external phase while the mixture was agitated for two hours at ambient temperature. The solid NS precipitated from the organic solvent, which evaporated at this stirring rate.

A vacuum pump and Buchner funnel equipment (Kennedy Manufacturing, USA) were employed to collect the prepared NS. Subsequently, it was cleaned thrice with distilled water and then dried for 12 h in a 40 °C oven imported from Germany (Mettler, Germany) [13, 14].

Table 1: Composition of various EC NSs loaded with ACEs

Formula	Ratio of ACE: EC	PVA conc.(w/v %)	RPM	Acetone (ml)	DCM (ml)**	DW (ml)**
F1	1:0.5	0.125	1000		5	50
F2	1:0.5	0.25	1000		5	50
F3	1:1	0.125	1000		5	50
F4	1:1	0.25	1000		5	50
F5	1:3	0.25	1000		5	50
F6	1:0.5	0.75	1000		5	50
F7	1:0.5	0.25	1250		5	50
F8	1:0.5	0.25	1500		5	50
F9	1:0.5	0.25	500		5	50
F10	1:0.5	0.25	1000	5		50

*All formulations were developed with 100 mg of ACE and a stirring duration of 2 h, **DW: distilled water, DCM: dichloromethane.

Characterization of NS

Proposed NS compositions underwent first evaluation testing. The physicochemical parameters encompass the quantification of:

PS and PDI

The vesicle size and dispersity were measured by Dynamic Light Scattering (DLS) at 90°θ using an ultra-zeta sizer, all measurements were performed in triplicate and expressed as Mean±Standard Deviation (M±SD, n=3). The PDI is calculated by dividing the SD by the mean droplet size and ranges from 0 to 1 [15].

Entrapment Efficiency %

The EE of a polymeric carrier is defined as the ratio of the drug mass actually trapped within the carrier to the initial drug loading. The following equation (1) is used to calculate it:

$$EE(\%) = \frac{\text{Actual loading}}{\text{Theoretical loading}} * 100 \dots \text{Eq. (1)}$$

The following (eq. 2) is the theoretical drug loading, which was determined by comparing the dosage of the medication with the total dosage and excipients utilized to make the NS:

$$\text{Theoretical loading (\%)} = \frac{\text{Total drug}}{\text{Total drug} + \text{Total excipients}} * 100 \dots \text{Eq. (2)}$$

For actual drug loading to make the NS, 10 mg of the dry-prepared NS loaded with the drug was mixed with 2 ml of distilled water. The mixture was then centrifuged at 13000 rpm for 20 min. After eliminating any solid particles, the remaining transparent liquid was tested for unbound ACE linked to the NS. An Ultra Violet-Visible (UV) spectrophotometer (Carry100 UV, Varian, Australia), was used to measure the amount of light absorbed at an ACE maximum absorbance wavelength (λ max.) of 273 nm. By mixing 10 mg of the dried powder with 10 ml of ethanol, the drug content in the NS could be measured. After that, a micro syringe filter with a pore size of 0.22 µm is used to pass the solution through after subjecting it to sonication. Analyzing the filtrate's absorbance with UV spectrophotometer allows one to determine whether ACE is present. To determine the real loading, the following equation (3) was used [16].

$$\text{Actual loading (\%)} = \frac{\text{Total drug} - \text{Free drug}}{\text{mg of dried powder}} * 100 \dots \text{Eq. (3)}$$

PY%

The PY% is calculated by dividing the dry formula weight by the total weight of the drug and polymer, as shown in equation (4) [17]:

$$PY\% = \frac{\text{Practical weight of nanosponge}}{\text{Theoretical weight (polymer + drug)}} * 100 \dots \text{Eq. (4)}$$

Then the optimum formula was investigated for:

FESEM

FESEM was employed to examine the surface morphology of the particles. The Zeiss-Gemini FESEM was used to analyze both the pure drug and the optimized NS formulation. Samples were sputtered with gold to make them conductive, and images were captured to provide detailed visualization of the surface topography and confirm the NS structure [18].

FTIR

FTIR was employed to confirm the chemical interactions between ACE and the polymeric matrix. The FTIR spectra were recorded using an FTIR 2500 instrument, scanning a range from 4000 to 400 cm⁻¹ with a resolution of 4 cm⁻¹. The analysis included the pure drug, a physical mixture of the drug and polymer, and the optimized NS formulation, ensuring the absence of chemical interactions that could affect the drug's stability [19].

DSC

DSC was utilized to study the thermal behavior of ACE and its compatibility with the excipients. Using a Shimadzu DSC-600, heat flow was measured as a function of temperature, ranging from 25 °C to 300 °C at a heating rate of 10 °C/min in a nitrogen atmosphere. The analysis was performed on the pure drug, the physical mixture of the drug and polymer, and the optimized NS formulation to determine the crystallinity and thermal stability [20].

Preparation of ACE hydrogel

In order to prepare the gel formulation, 70% of the total needed weight of D. W. was heated to 70 °C. Subsequently, HPMC-K100

powder (at different concentrations: 1%, 1.5%, 2%) was gradually added and evenly distributed in the preheated D. W. The final mixture was agitated until a uniform dispersion was achieved. To facilitate polymer swelling, the aqueous dispersion of HPMC-K100 was left undisturbed overnight. The remaining formulation components, including PolyEthylene Glycol 400 (PEG400) at different concentrations (5%, 7.5%, and 10%), which serves as a

humectant and viscosity modifier, together with the active ingredients (either the ACE or the ACE NS equivalent to 1% w/w ACE) and the D. W. to reach the final weight, were added to the solution. The solution was homogenized at 700 RPM. The gel was left undisturbed overnight to eliminate trapped air bubbles, and a sealed glass container was used to keep the gel that was made [21]. All hydrogel compositions are listed in table 2.

Table 2: ACE-NS-hydrogel compositions

Formula	NS equivalent to ACE%	Pure ACE%	HPMC-K100%	PEG400%	D. W. up to(g)
G1	1		2	10	100
G2	1		2	7.5	100
G3	1		2	5	100
G4	1		1	10	100
G5	1		1	7.5	100
G6	1		1	5	100
G7	1		1.5	7.5	100
G-plain		1	2	10	100

Evaluation of the prepared hydrogel

The visual examination

The evaluation assessed several visual attributes, including uniformity, color, and homogeneity [22].

Measurement of pH

Human skin is acidic, contributes to bodily defense, and prevents the degradation of stratum corneum integrity [23, 24]. Skin pH fluctuates due to various causes including illness, detergents, aging, and sweat constituents [25]. Consequently, the skin pH possesses critical characteristics that must be confirmed such that the formulation is safe and irritation is minimized. One g of the gel was introduced into 10 ml of D. W. and subjected to sonication for five minutes [26]. The pH of the gel was measured utilizing a meter manufactured by Hanna, Nus, Falau, Romania. The procedure was conducted in 3 times.

Determination of Drug content

Precisely weighed (1g) ACE-NS hydrogels, being equivalent to 10 mg of ACE, were placed in a 50 volumetric flask filled with phosphate-buffered saline at a pH of 7.4. Following a 30 min sonication torsion, the solution was allowed to rest overnight. The medication's concentration was determined by quantifying the absorbance at 272 nm as measured by an UV spectrophotometer (Carry100 UV, Varian, Australia [27].

Determination of spreadability

Hydrogel weighing 1g was positioned between two glass plates measuring 14x14 cm. A load weighing (500 g) was positioned on the top glass plate. Following a five minute waiting period, the diameter was measured and recorded. The hydrogel spreading mechanism was shown to result in an increase in diameter [28].

Viscosity determination

At room temperature viscosity and rheological behavior of the hydrogel compositions were evaluated using a spindle no. 7. The speed of rotation was increased from 0 to 200. The test was done using a viscometer (Myr VR3000, Visotech, Spain) [29].

In vitro permeation test

The Franz diffusion cell with an effective diffusion area of 1.767 cm² was used to conduct *in vitro* permeation tests on all hydrogel compositions permeating (Strat-M®) Membrane [30]. In order to establish a sink condition, 12 ml of Phosphate Buffer Saline pH 7.4 (PBS) was introduced into the receptor compartment. This decision was made based on our previous investigation of ACE saturation solubility in PBS, which revealed a solubility of 13.05±0.15 mg/ml. Next, a Strat-M® Membrane was placed in the space between the donor and receptor compartments. With the stirring speed set at 600 RPM and the temperature kept at 37±0.5 °C, we let the membrane's temperature stabilize for a duration of 15 min.

Thereafter, a quantity of 1g (equal to 10 mg of ACE)-NS Hydrogels or the plain Hydrogel was added to the donor part. At regular time periods of 0.25, 0.5, 1, 2, 3, 4, 5, 6, 7, and 8 h, 1 ml of the receptor compartment was withdrawn and substituted with fresh PBS to ensure a consistent solubility state. In order to quantify the amounts of ACE that penetrated during each time interval, the absorbance at the maximum wavelength of ACE in PBS was measured using spectrophotometry. Permeation testing was conducted using Strat-M® Membrane due to its strong connection with permeation research with human body skin [31]. The operation was executed three times, and the total quantity of ACE that permeated was computed as follows:

The cumulative ACE amount = $V_R \times C_n + [V_s (\sum C_1 + C_2 + \dots + C_{n-1})]$ Eq. (5)

Denoted as V_R , the receptor volume, V_s represents the volume of withdrawal samples each time, and C_n represents the sample concentration at the nth time. To determine the permeation in µg/cm², the computed cumulative amount was then divided by the surface area of the Franz in cm². The slope was used to calculate the steady-state flow (J_{ss}) after graphing the cumulative ACE penetrated per unit area and time (µg/cm²/h). Additionally, the coefficient of permeability (K_p) was determined by formulating a ratio of flow to the starting concentration of ACE in the ACE-NS-hydrogel in the donor compartment [32]. The permeability coefficient (K_p) was determined using the following equation:

$$K_p = \frac{J_{ss}}{C_0} \dots \dots \text{Eq. (6)}$$

Given the initial concentration of the medicine in the donor section, denoted as C_0 , the steady condition flow is represented by J_{ss} , and the apparent penetration coefficient is denoted as K_p [33].

In vitro release investigation

This study investigated *in vitro* drug dissolution of the optimum ACE-NS-Hydrogel formulation. The release after eight hours was determined using the dialysis bag technique [34]. From the selected ACE-NS-Hydrogel formulation and plain hydrogel, one g of the gel (equal to 10 mg of ACE) was extracted and added to dialysis bags that had been immersed in the release media overnight. The dialysis bags were placed in a paddle-style (type II-dissolving equipment) containing 250 ml of a PBS solution as the release medium. The paddles rotated at a speed of 100 RPM, while the overall temperature of the system was kept at 37±0.2 °C. At set time intervals of 5, 10, 15, 30 min, and 1, 2, 3, 4, 5, 6, 7, 8hr, 5 milliliters were withdrawn and substituted with a fresh PBS. The samples were filtered via a 0.22 µm filter syringe and subsequently tested for ACE concentration using a double-beam UV-visible spectrophotometer at its λ_{max} of ACE at 272 [35].

In vivo anti-inflammatory study

The ethical committee of the Iraqi Ministry of Scientific Research and Higher Education at the University of Baghdad, College of Pharmacy (permission number: RECAUBCP3102023K), accepted the animal model employed in the study. An albumin-induced

paw in rat's edema was used as an animal model for investigation of the anti-inflammatory impact of ACE following topical administration. Acute inflammation and edema induced by albumin commenced after 30 min [36]. Nine adult female albino rats, with an average weight of 150 ± 25 g (prepared by the College of Veterinary Medicine at the University of Baghdad), were randomly allocated into three groups: control, ACE-NS hydrogel (G1), and plain ACE-hydrogel (G-P), each consisting of three rats. Except for the control group, the dorsal region of the rats was shaved 24 h prior to the onset of the trials.

To induce paw swelling, 0.1 ml of fresh egg albumin was injected into the right paws and should be administered 30 min prior to treatment with hydrogel. 0.5 g of Treatments G1 and (G-P) were administered to the shaved dorsal area of all animals, except for the control group. Measurements of paw volume were taken at 1, 2, 3, 4, and 24 h. Post-injection using a Vernier caliper and reported as a percentage of the original hind paw volume. The edema inhibition % was determined using the following equation:

$$\% \text{ Inhibition of edema } \% = S_0 - S_t / S_0 \dots \text{Eq. (7)}$$

Where the treatment group's edema size is S_t , and S_0 is the control group.

Study the impact of temperature on stability

The optimized hydrogel formula was maintained at room temperature (30°C) and in a refrigerator at (4°C) for a period of three months. After three months, a sample was evaluated for physical appearance, pH, drug content, and *in vitro* drug release profile. This stability testing follows the guidelines outlined in ICH Q1A (R2), which provides recommendations on stability testing protocols, including temperature, humidity, and trial duration for different climatic zones [37].

Statistical analysis

Analyzed using one-way ANOVA to determine statistical significance, followed by post-hoc Tukey tests to compare group means. Power analysis was conducted to ensure adequate sample sizes, providing a power of 0.8 to detect significant differences at a significance threshold of $P < 0.05$, the results of the studies were reported as the mean of triplicate samples \pm SD [38].

RESULTS AND DISCUSSION

Evaluation of NS

DCM was selected as the internal phase organic solvent due to its affinity for both the drug and the polymer, as well as its rapid evaporation after diffusion, resulting in the formation of solid ACE NSs. The emulsion solvent diffusion technique was employed because of its simplicity in execution [39].

Table 3: The statistical characteristics of NS, which included the PY%, EE%, PDI, and PS

Formula code	PY% \pm SD	EE% \pm SD	PS \pm SD (nm)	PDI \pm SD
F1	76.74 \pm 3.1	87.9 \pm 3.6	87.06 \pm 2.9	0.47 \pm 0.005
F2	77.92 \pm 2.2	90.05 \pm 1.1	127.3 \pm 3.2	0.1 \pm 0.02
F3	74.44 \pm 5.09	53.4 \pm 2.7	292.7 \pm 79.01	0.49 \pm 0.15
F4	74.66 \pm 7.05	74.8 \pm 2.2	694.7 \pm 16.5	0.57 \pm 0.006
F5	68.66 \pm 2.8	44.3 \pm 3.9	923.3 \pm 113.03	1 \pm 0.1
F6	75.25 \pm 4.8	52.5 \pm 0.7	1815.3 \pm 460.8	1.04 \pm 0.27
F7	75.25 \pm 2.2	67.3 \pm 0.9	98.03 \pm 2.9	0.55 \pm 0.01
F8	74.96 \pm 2.05	60.2 \pm 1.8	80.5 \pm 1.6	0.55 \pm 0.004
F9	75.25 \pm 3.5	74.7 \pm 1.9	1832 \pm 346.08	1.09 \pm 0.14
F10	76.14 \pm 2.2	35.6 \pm 2.5	894.3 \pm 32.3	0.28 \pm 0.02

n=3

Table 3 demonstrates that the percentage of ACE entrapment exhibited similar patterns to the PY%. Specifically, when the polymer: drug ratio was increased, there was a significant reduction ($p < 0.05$) in the PY% from 77.92 \pm 2.2% to 68.66 \pm 2.8% and in the percentage of ACE EE% from 90.05 \pm 1.1% to 44.3 \pm 3.9% for formula F2 and F5, respectively. This phenomenon can be elucidated by the observation that reducing the quantity of polymer simultaneously results in an increase in the quantity of drug introduced, thereby causing a reduction in the viscosity of the medium. This, in turn, facilitates the diffusion of the drug moiety and the development of a more pliable polymer layer, thus enhancing the EE% [40]. Conversely, as the ratio of polymer to drug proportion rises, the PS will also increase. This is because a higher ratio of polymer to drug results in a greater quantity of the polymer accessible for the synthesis of ACE-NS. Consequently, the thickness of the polymer increases, leading to the production of larger-size NS [41]. Smaller PSs generally result in increased surface area available for drug loading, which can lead to higher EE% and PY%. A higher surface area allows more drug molecules to be adsorbed or encapsulated within the nanoparticle matrix, the

obtained results were inconsistent with that obtained by Patel *et al.*, 2020; Zhang *et al.*, 2020 [42, 43].

Selecting the optimal formulation

For subsequent testing, the NS formulation exhibiting the optimal characteristics of minimal PS distribution, satisfactory PY%, and maximal drug EE% was selected. Consequently, the formula F2 from table 3 was chosen. The enhanced stability and solubility of ACE in this study are due to the high surface porosity of the NSs, which increases the surface area for drug loading and controlled release. This structural feature ensures a more consistent and effective drug delivery [44].

FESEM

The findings of a FESEM morphological examination of (F2) are shown, in comparison to ACE pure powder. Fig. 1 the NSs embedded with ACE exhibited tiny particles with approximately rough round in shape as illustrated in fig. 2 the rough and porous surface of NS was a result of the diffusion of DCM from the surface [45].

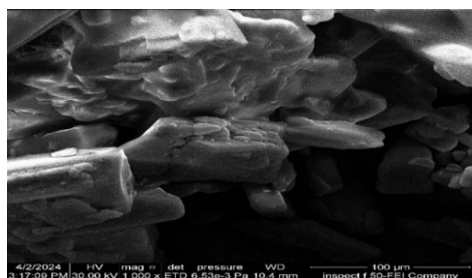


Fig. 1: FESEM of ACE at 1000X magnification

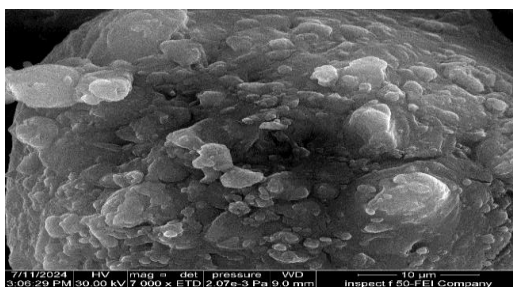


Fig. 2: FESEM of formula (F2); at 7.00Kx magnification

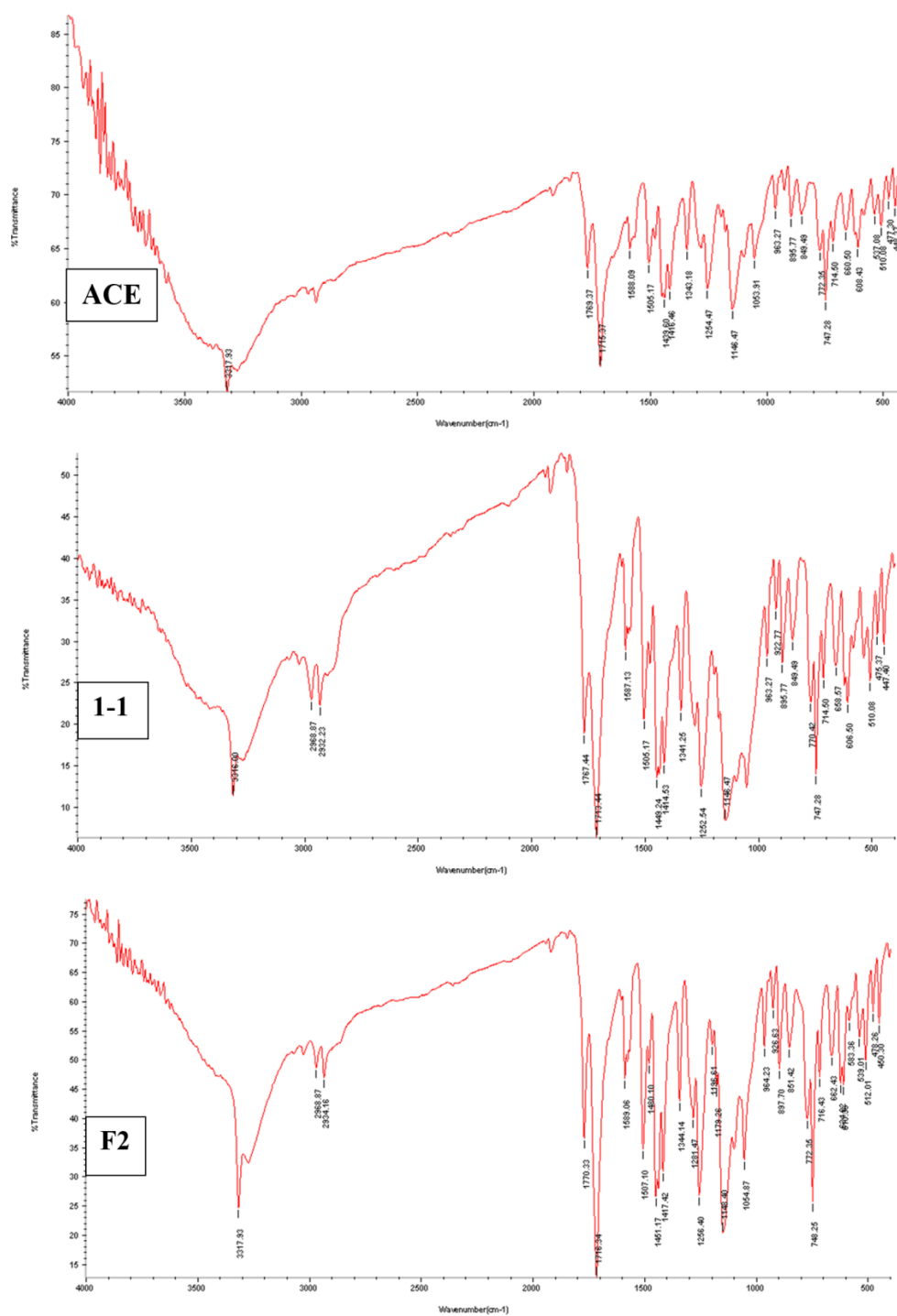


Fig. 3: The FTIR spectra for pure ACE powder, physical mixture (1-1), and F2

FTIR

Here are the features of the absorption bands of ACE: for N-H or O-H stretching, 3317 cm^{-1} , 2934 cm^{-1} for C-H stretching (aromatic and aliphatic stretching vibrations, respectively), 3277 cm^{-1} , for C=O stretching, 1771 cm^{-1} , and for C=C stretching of aromatic compounds, 1585 cm^{-1} and 1506 cm^{-1} . Fig. 3 offers additional information on the noticeable bands. There was no evidence of drug-polymer interaction since the ACE peaks in the prepared NS

did not differ significantly from those in the pure drug with no appearance of new peaks or major shifting of the drug characteristic peaks [46].

DSC

The DSC thermogram of pure ACE exhibited a distinct endothermic peak at $148.51\text{ }^{\circ}\text{C}$ which corresponds to the melting point of pure ACE in its crystalline state fig. 4.

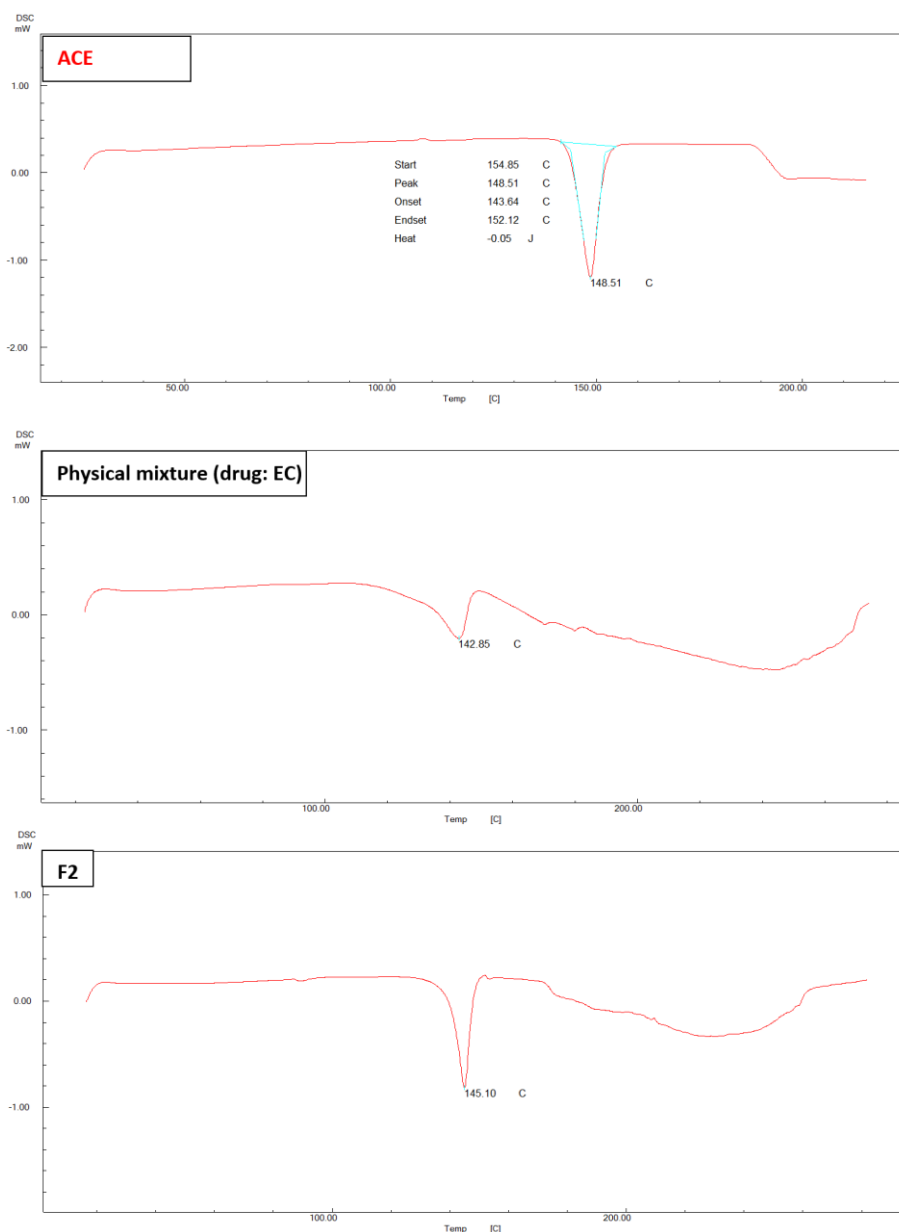


Fig. 4: DSC thermogram of pure ACE, physical mixture, and (F2) NS

In fig. 4, it is evident that the endothermic peak of ACE in the physical mixture has undergone a displacement towards a reduced melting point of $142.85\text{ }^{\circ}\text{C}$. The DSC thermogram of the chosen formula (F2) exhibits a depressed endotherm of the drug at a lower melting point of $145.10\text{ }^{\circ}\text{C}$, leading to a comparatively less crystalline structure [47].

Evaluation of the prepared hydrogel

The visual examination

Visual examination of the physical characteristics of all the ACE-NS hydrogels produced showed that the formulations exhibited

excellent uniformity, absence of any roughness, a light white color, and no occurrence of phase separation.

pH determination

All synthesized hydrogels have a pH within the range of 6 ± 0.14 to 6.5 ± 0.14 , which closely approximates the pH of the skin. This pH range is well-established in the literature and does not cause any irritation or itching when applied [48].

Determination of DC

Table 4 presents the reported ACE content data for all the ACE-NS hydrogels that were produced. The actual DC quantified varied

between $89.3 \pm 0.18\%$ and $95.19 \pm 0.23\%$ of the theoretical quantity. The homogeneous distribution of ACE-NS throughout the hydrogel structure was proven.

Spreadability

Hydrogel spreadability is the degree to which the hydrogel disperses over the skin when applied. As the polymer concentration increases, the spreadability of the hydrogel diminishes. Table 4 presented data of spreadability measurements.

Determination of the viscosity

As illustrated in fig. 5, as the shear rate increased, the viscosity of the gel decreased, indicating a shear-thinning pseudo plastic flow characteristic. Pseudo plasticity is desirable for topical gels because it ensures ease of spreading when applied to the skin, as the viscosity decreases under shear stress such as during

application [49]. The results indicated that HPMC exhibited effective gelling properties in the production of hydrogels, making it a suitable choice for formulating stable and user-friendly topical products. Comparing the viscosity to benchmarks for similar topical formulations, the values obtained for the HPMC hydrogel fall within the acceptable range, indicating its practical application for efficient drug delivery [50].

In vitro permeation study

The hydrogel formulations undergo *in vitro* permeation testing, and the outcomes of the transdermal permeation through (Strat-M®) from various formulations are presented in fig. 6. The flux, permeability coefficient, and Permeation Enhancement (PE) values obtained for various formulations are presented in table 5. The release profile demonstrated that the drug release from each formulation was influenced by the concentration of polymers, HPMC-K100 and PEG400.

Table 4: pH Data, DC, and spreadability of hydrogels loaded with ACE-NS

Formula code	PH \pm SD	DC% \pm SD	Spreadable diameter (cm) \pm SD
G1	6.2 \pm 0.15	95.19 \pm 0.23	9.5 \pm 0.2
G2	6.3 \pm 0.14	93.15 \pm 0.31	7.7 \pm 0.15
G3	6.0 \pm 0.12	93.61 \pm 0.21	9 \pm 0.2
G4	6.4 \pm 0.13	91.9 \pm 0.41	11.7 \pm 0.25
G5	6.5 \pm 0.14	93.45 \pm 0.31	13.8 \pm 0.3
G6	6.2 \pm 0.12	92.33 \pm 0.26	13.2 \pm 0.2
G7	6.5 \pm 0.2	89.3 \pm 0.18	10.7 \pm 0.15
G-plain	6 \pm 0.14	90.55 \pm 0.27	13 \pm 0.15

n=3

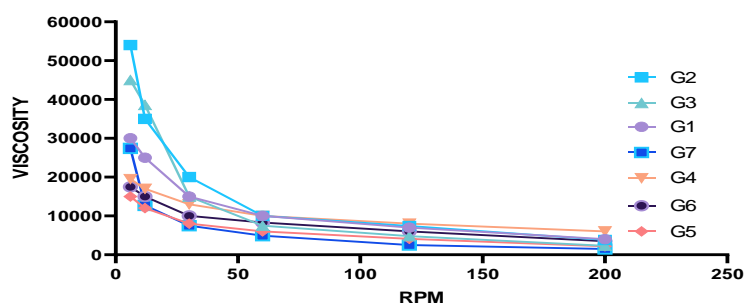


Fig. 5: Viscosity analysis of ACE-NS hydrogels

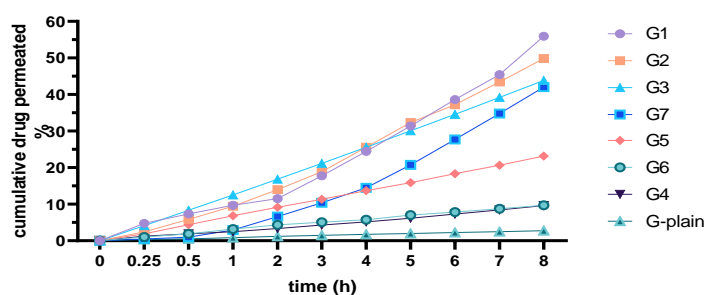


Fig. 6: Ex-vivo permeation profiles of all formulated transdermal hydrogels of ACE

Table 5: The permeation parameters of the ACE-NS hydrogel and plain hydrogel

Formula code	Flux ($\mu\text{g}/\text{cm}^2/\text{h}$) \pm SD	Permeability coefficient ($\text{cm}/\text{h} \times 10^{-2}$) \pm SD	Permeation-enhanced ratio
G1	723.93 \pm 5.1	7.23 \pm 0.5	28.8
G2	600.9 \pm 4.8	6 \pm 0.3	23.9
G3	601.24 \pm 5.6	6.01 \pm 0.3	23.91
G4	91.14 \pm 3.2	0.91 \pm 0.08	3.62
G5	104.41 \pm 3.7	1.04 \pm 0.02	4.15
G6	450.71 \pm 5.9	4.5 \pm 0.09	17.92
G7	232.9 \pm 5.1	2.32 \pm 0.05	9.26
G-plain	25.14 \pm 1.9	0.25 \pm 0.01	-----

n=3

A statistical analysis of the flux over a period of 8 h revealed that the ACE-NS-hydrogel preparations G1 exhibited the highest cumulative penetration rate of $55.94 \pm 1.4\%$ among all the preparations, while G-plain of ACE exhibited cumulative penetration rates of $2.73 \pm 0.3\%$ at 8 h. The ratio of PE of G1 (28.8), derived from the subsequent equation:

$$PE = J_{ss} (\text{ACE-NS-of gel}) / J_{ss} \text{ of ACE plain gel} \dots \text{Eq... (8)}$$

PE is the quantitative measure of the permeation enhancement, while J_{ss} represents the flux of ACE-NS and plain hydrogel [51]. The significantly higher ($p < 0.05$) penetration rate and permeability coefficient for the ACE-NS hydrogel (G1) compared to the plain ACE hydrogel (G-plain) suggest that the NS formulation substantially enhances drug permeation through the skin. This improvement can be attributed to the smaller PS and increased surface area of the NSs, which facilitate better interaction with the skin and more efficient drug delivery [52]. Recent studies have reported similar findings with other NSAID-loaded NSs. For example, a study by Gupta *et al.* (2022) found that a NS formulation of Diclofenac exhibited a cumulative penetration rate of $48.7 \pm 2.1\%$ over 8 h, significantly higher than the plain Diclofenac gel, which had a penetration rate of $3.1 \pm 0.2\%$. Another study by Liu *et al.* (2024) on Ibuprofen NSs reported a permeability coefficient of $6.95 \pm 0.45 \text{ cm/h} \times 10^{-2}$, indicating that NS formulations generally exhibit higher permeation rates compared to traditional hydrogels [53, 54]. The permeability coefficient was evaluated using the Strat-M® membrane, a synthetic, non-animal-based model for transdermal diffusion testing. Strat-M® membrane is designed to mimic human skin permeability and is predictive of diffusion in human skin for a wide range of compounds and formulations [1]. This model provides consistent and reliable data without the variability associated with biological skin models [55].

In vitro drug release study

The drug release investigation was conducted *in vitro* using phosphate buffer at a pH of 7.4. The release pattern of the medication from the

synthesized hydrogels is shown in fig. 7. During the 8 h release assay, the drug release of the gel of G1 had a percentage of $84.5 \pm 3.8\%$, whereas the plain hydrogel had a percentage of $24.8 \pm 4.2\%$. There was a statistically significant difference ($p < 0.05$) between G1 hydrogel and plain hydrogel. This difference can be attributed to the enhanced dissolving rate and permeation resulting from the smaller size of the NS. Due to the reduced size of drug particles, the Noyes-Whitney equation requires a larger surface area, resulting in a substantial elevation area for the NS. Moreover, the diffusion distance shortens for particles of extremely small size. Therefore, the elevated surface area and the concomitant reduction in diffusion distance could greatly enhance the rate of dissolution of the drug [56].

The results were compared with existing NS-based hydrogels used for other NSAIDs, such as ibuprofen and ketoprofen. The results demonstrated superior drug EE% and release profile, highlighting the potential advantages of our formulation. Specifically, our ACE-loaded NS showed a more consistent and prolonged drug release compared to the existing formulations by Farsana P and Chandur VK, which can lead to improved therapeutic outcomes [57, 58].

In vivo anti-inflammatory-activity

Fig. 8 demonstrated that formula G1-Hydrogel showed a substantial effect ($p\text{-value} < 0.0001$). Inhibited the inflammation by $65.38 \pm 1.1\%$ for the duration of 24 h. Conversely, the inhibition of ACE-Plain hydrogel was $24.23 \pm 0.95\%$. The NS hydrogel performs better primarily due to its superior skin penetration and longer drug retention in the affected area. The NS formulation enhances drug permeation through the skin, attributed to the smaller PS and increased surface area of the NSs, which facilitate better interaction with the skin. Additionally, the controlled release mechanism of the NSs ensures prolonged drug retention at the site of inflammation, leading to more effective and sustained therapeutic effects [59]. Throughout the experiment, no rats exhibited irritation, erythema, or lesions following hydrogel treatment as depicted in fig. 9.

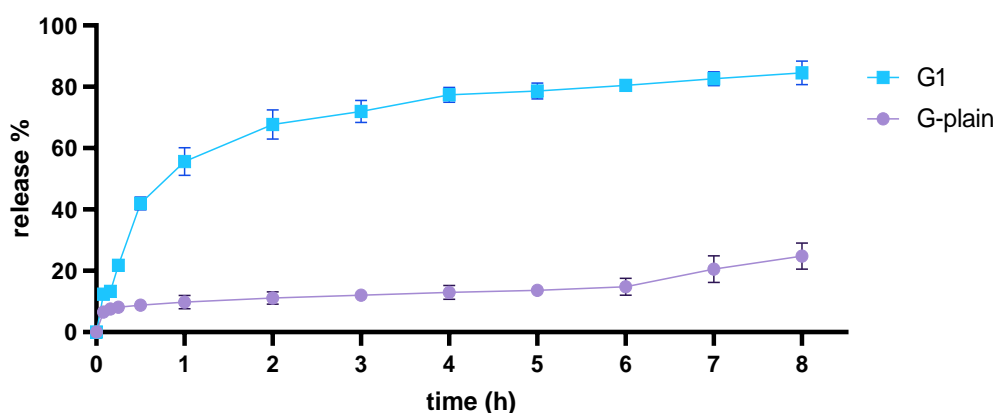


Fig. 7: In vitro drug dissolution of G1-hydrogel and ACE-plain hydrogel

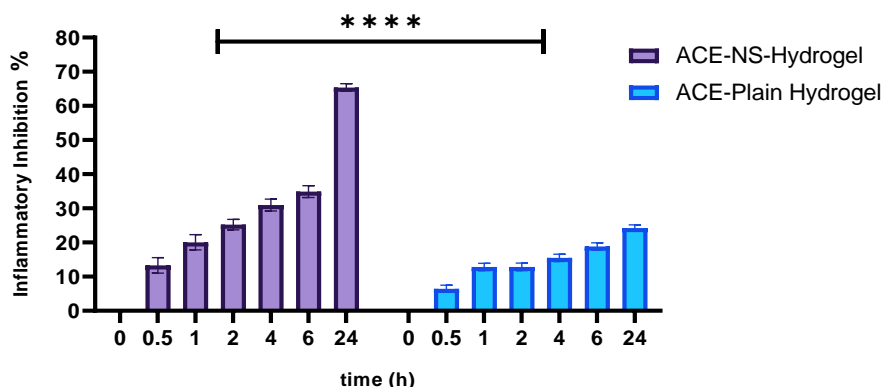


Fig. (8): Inflammatory inhibition% of ACE-NS- hydrogel and ACE plain hydrogel, (**** indicates a $p\text{-value} < 0.0001$)



Fig. 9: One rat of the G1 group after A) 1 h and B) 24 h

Table 6: Effect of storage temperature 30 °C and 4 °C after 3 Mo on G1

Parameters	Results		
	Initial \pm SD	Stored at 4 °C \pm SD	Stored at 30 °C \pm SD
PH	6.2 \pm 0.15	6.1 \pm 0.6	6.2 \pm 0.4
DC%	95.19 \pm 0.23	95 \pm 0.4	94.2 \pm 0.5

n=3

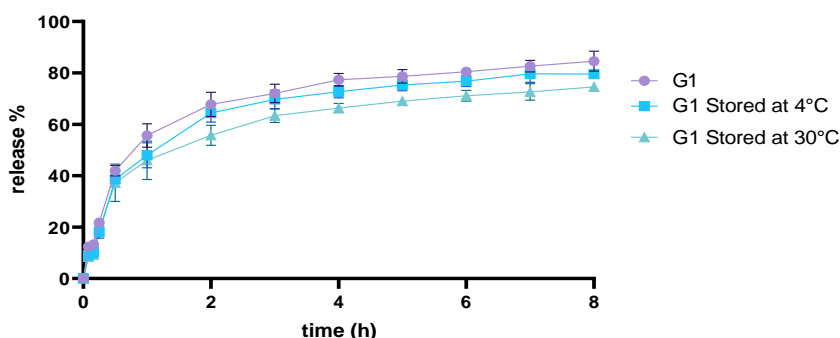


Fig. 10: Release profile of G1 after three months of storage at 30 °C and 4 °C

Stability study

The chosen ACE NS loaded EC hydrogel formulation exhibited no significant differences ($p>0.05$) in physical appearance, pH, DC, and *in vitro* drug release profile as illustrated in fig. 10 after being stored at 30 °C and in a refrigerator at 4 °C for three months [60]. The outcomes of stability investigations are presented in table 6.

CONCLUSION

The data demonstrate that emulsion solvent diffusion technique is an efficient and cost-effective method for the preparation of drug nanoparticles, and it is simple to implement in drug nanoparticle manufacturing. The data indicate that the dissolution is enhanced when ACE particles are at the nanoscale. The ACE-NS-based hydrogel exhibited an improved drug release rate in comparison to the blank hydrogel. These findings suggest that the NS-loaded hydrogel approach can be extended beyond ACE to other poorly soluble drugs. This technology holds promise for targeted therapies in inflammatory diseases. Future clinical development stages will involve more extensive *in vivo* studies and eventual clinical trials. While no direct comparisons were made in this study, the NS hydrogel formulation has potential commercial advantages over existing ACE gels. These advantages include reduced dosing frequency and improved patient compliance. The enhanced skin penetration and prolonged drug retention provided by the NS

formulation could lead to more effective and sustained therapeutic effects, making it a promising alternative to current commercial options.

ACKNOWLEDGMENT

The authors express their gratitude to the College of Pharmacy, the University of Baghdad, and the Department of Pharmaceutics for their educational supervision.

FUNDING

This research received no external funding.

AUTHORS CONTRIBUTIONS

Concept–Lubna A. Sabri; Design–Mays Hassan, LS; Supervision–LS; Resources–MH; Materials–MH; Data Collection and/or Processing–MH; Analysis and/or Interpretation MH, LS; Literature Search–MH, LS; Writing–MH; Critical Reviews–LS.

CONFLICT OF INTERESTS

The authors declared no conflict of interest in the manuscript

REFERENCES

- Lo HJ. Two genes linked to rheumatoid arthritis and osteoporosis could serve as targets for diagnosis and treatment. *APL Bioeng.* 2024;12(3):123-34.

2. Gupta P, Sharma R, Kumar V. NSs: an innovative approach in drug delivery and environmental cleanup. *J Drug Deliv Sci Technol.* 2023;76:103791.
3. Zhou Y, Zhang Y, Lin W. Advanced NSs for targeted drug delivery: recent updates and future perspectives. *J Nanobiotechnol.* 2023;21(1):94-108.
4. Ahmed A, Ali S, Khan H. Synthesis of NS formulations using emulsion solvent diffusion: evaluation and characterization. *Int J Pharm.* 2023;618:121583.
5. Liu Y, Wang J, Zhang X. Optimization of NSs for drug delivery using emulsion solvent diffusion technique. *J Drug Deliv Sci Technol.* 2024;78:103932.
6. Dave V, Yadav S, Sharma S, Panwar N. Guggulusome-a novel vesicular carrier. *Iraqi J Pharm Sci.* 2014;23:73-82.
7. Alezzy AAE, Al-Khedairy EBH. Preparation and evaluation of ACE solid dispersion. *Res J Pharm Technol.* 2023;16:5358-65.
8. Koshy S, George C, Abraham S. Development and characterization of ACE-loaded NS gel for the management of rheumatoid arthritis. *Asian J Pharm Clin Res.* 2024;15(3):123-30.
9. Gupta M, Shrivastava B, Ghuge A, Dand N. Formulation and evaluation of NS-based drug delivery system of ACE for topical application. *Res J Pharm Technol.* 2023;16(12):5713-21.
10. Tiwari K, Bhattacharya S. The ascension of nanosponges as a drug delivery carrier: preparation, characterization, and applications. *J Mater Sci Mater Med.* 2022;33(3):28. doi: [10.1007/s10856-022-06652-9](https://doi.org/10.1007/s10856-022-06652-9), PMID [35244808](https://pubmed.ncbi.nlm.nih.gov/35244808/).
11. Tiwari A, Tiwari V, Palaria B, Kumar M, Kaushik D. Microsponges: a breakthrough tool in pharmaceutical research. *Futur J Pharm Sci.* 2022;8(1):31. doi: [10.1186/s43094-022-00421-9](https://doi.org/10.1186/s43094-022-00421-9).
12. Ahmed SA, Lubna AS. Formulation variables affecting clobetasol microsponges properties. *Iraqi J Pharm Sci.* 2023;32 Suppl:225-34.
13. Abass MM, A Rajab N. Preparation and characterization of etodolac as a topical nanosponges hydrogel. *Iraqi J Pharm Sci.* 2019;28(1):64-74. doi: [10.31351/vol28iss1pp64-74](https://doi.org/10.31351/vol28iss1pp64-74).
14. Chaudhary S, Mehta P, Kulkarni P. Formulation and characterization of ACE-loaded NSs using emulsion solvent diffusion method. *Int J Pharm Sci Rev Res.* 2023;52(1):100-9.
15. Mohammed BS, Al-Gawhari FJ. Preparation of posaconazole nanosponges for improved topical delivery system. *Int J Drug Deliv Technol.* 2022;12(1):8-14. doi: [10.25258/ijddt.12.1.2](https://doi.org/10.25258/ijddt.12.1.2).
16. Saini R, Sharma P, Singh G, Kaur N, Kaur G. Formulation and evaluation of ACE-loaded NSs for improved drug delivery. *Int J Pharm Sci Res.* 2023;14(5):1234-42.
17. Salman AH, Al-Gawhari FJ, Al-kinani KK. The effect of formulation and process variables on prepared etoricoxib nanosponges. *J Adv Pharm Educ Res.* 2021;11(2):82-7. doi: [10.51847/Q0QRKUV2kQ](https://doi.org/10.51847/Q0QRKUV2kQ).
18. Mancini M, Cerroni L, Palopoli P, Olivi G, Olivi M, Buoni C. FESEM evaluation of smear layer removal from conservatively shaped canals: laser activated irrigation (PIPS and SWEEPS) compared to sonic and passive ultrasonic activation-an ex vivo study. *BMC Oral Health.* 2021;21(1):81. doi: [10.1186/s12903-021-01427-0](https://doi.org/10.1186/s12903-021-01427-0), PMID [33618701](https://pubmed.ncbi.nlm.nih.gov/33618701/).
19. Moin A, Roohi NK, Rizvi SM, Ashraf SA, Siddiqui AJ, Patel M. Design and formulation of polymeric nanosponge tablets with enhanced solubility for combination therapy. *RSC Adv.* 2020;10(57):34869-84. doi: [10.1039/d0ra06611g](https://doi.org/10.1039/d0ra06611g), PMID [35514416](https://pubmed.ncbi.nlm.nih.gov/35514416/).
20. Patel T, Amin A. Design and formulation of polymeric NS tablets with enhanced solubility for combination therapy. *Int J Appl Pharm.* 2020;12(2):45-53.
21. Kumar A, Sharma M, Kaur R, Singh G. Formulation and evaluation of ACE-loaded NSs for improved drug delivery. *Int J Pharm Sci Res.* 2023;14(5):1234-42.
22. Ghosh S, Banerjee R, Mandal A. Physicochemical characterization and stability studies of a new topical gel formulation. *Int J Pharm Sci Res.* 2023;14(6):2451-61.
23. Saad Hameed A, Sabri LA. Preparation and in-vitro evaluation of carbopol hydrogel of clobetasol-loaded ethylcellulose microsponges. *JRP.* 2024;28(5):1619-31. doi: [10.29228/jrp.839](https://doi.org/10.29228/jrp.839).
24. Shakshouk H, Gibson LE. Cutaneous manifestations of ANCA-associated vasculitis: a retrospective review of 211 cases with emphasis on clinicopathologic correlation and ANCA status. *Int J Dermatol.* 2023;62(2):231-8. doi: [10.1111/ijd.16214](https://doi.org/10.1111/ijd.16214), PMID [35576100](https://pubmed.ncbi.nlm.nih.gov/35576100/).
25. Zhu W, Gao Y, Tan X, Huang Y. Factors influencing skin pH: a review. *Skin Pharmacol Physiol.* 2024;37(3):157-69.
26. Kasparaviciene G, Maslii Y, Herbina N, Kazlauskienė D, Markska M, Bernatoniene J. Development and evaluation of two-phase gel formulations for enhanced delivery of active ingredients: sodium diclofenac and camphor. *Pharmaceutics.* 2024;16(3):366. doi: [10.3390/pharmaceutics16030366](https://doi.org/10.3390/pharmaceutics16030366), PMID [38543261](https://pubmed.ncbi.nlm.nih.gov/38543261/).
27. Al-Mansoori MK, Sabri LA. Preparation and evaluation of transdermal gel loaded with plastics containing meloxicam. *J Res Pharm.* 2024;28(4):1200-9.
28. Purohit AA, Chavan DU, Marques SM, DCruz CE, Kumar L, Bhide PJ. Formulation and evaluation of a novel cubosomal emulgel for topical delivery of luliconazole. *Tenside Surfactants Detergents.* 2022;59(5):373-82. doi: [10.1515/tsd-2022-2442](https://doi.org/10.1515/tsd-2022-2442).
29. Sadeq ZA, Mohammed MF. Preparation and *in vitro* evaluation of topical gel of 5-fluorouracil. *J Adv Pharm Educ Res.* 2021;11(4):80-5. doi: [10.51847/ycPsBAy4RG](https://doi.org/10.51847/ycPsBAy4RG).
30. Patel S, Anderson C, Salvi D. Evaluation of novel hydrogel formulations using the Franz diffusion cell method. *Int J Pharm Sci Rev Res.* 2023;23(6):521-9.
31. Al-Ameri AA, Al-Gawhari FJ. Formulation development of meloxicam binary ethosomal hydrogel for topical delivery: *in vitro* and *in vivo* assessment. *Pharmaceutics.* 2024;16(7):898. doi: [10.3390/pharmaceutics16070898](https://doi.org/10.3390/pharmaceutics16070898), PMID [39065595](https://pubmed.ncbi.nlm.nih.gov/39065595/).
32. Rao MT, Rao YS, Ratna J V, Kumari Pv K. Characterization and ex vivo studies of nanoparticle incorporated transdermal patch of itraconazole. *Indian J Pharm Sci.* 2020;82(5):799-808. doi: [10.36468/pharmaceutical-sciences.708](https://doi.org/10.36468/pharmaceutical-sciences.708).
33. Hnin HM, Stefánsson E, Loftsson T, Asasutjarit R, Charnvanich D, Jansook P. Physicochemical and stability evaluation of topical niosomal encapsulating fosinopril/γ-cyclodextrin complex for ocular delivery. *Pharmaceutics.* 2022;14(6):1147. doi: [10.3390/pharmaceutics14061147](https://doi.org/10.3390/pharmaceutics14061147), PMID [35745720](https://pubmed.ncbi.nlm.nih.gov/35745720/).
34. Mitra A, Thakur RS, Chakraborty S. Evaluation of the *in vitro* drug release profile of NS hydrogel formulations using the dialysis bag method. *Int J Pharm Sci Rev Res.* 2023;23(6):450-8.
35. Chakraborty S, Thakur RS, Mitra A. Evaluation of *in vitro* drug release profile of NS hydrogel formulations using the dialysis bag method. *Int J Pharm Sci Rev Res.* 2023;23(6):450-8.
36. Barung EN, Dumanauw JM, Duri MF, Kalonio DE. Egg white-induced inflammation models: a study of edema profile and histological change of rat's paw. *J Adv Pharm Technol Res.* 2021;12(2):109-12. doi: [10.4103/japtr.JAPTR_262_20](https://doi.org/10.4103/japtr.JAPTR_262_20), PMID [34159139](https://pubmed.ncbi.nlm.nih.gov/34159139/).
37. Khan R, Patel S, Desai A. Stability studies on NSs-based hydrogel formulations: evaluation of physical and chemical properties. *J Pharm Sci Res.* 2023;15(7):842-9.
38. Sharma A, Gupta P, Kaur R. NSs: a comprehensive review. *Int J Curr Pharm Rev Res.* 2024;6(1):60-70.
39. Ahmed A, Khan R, Desai A. Solvent selection and process optimization for the synthesis of drug-loaded NSs using emulsion solvent diffusion. *J Pharm Biomed Anal.* 2023;212:114657.
40. Yehia RM, Attia DA, Elmazar MM, El-Nabarawi MA, Teaima MH. Screening of adapalene microsponges fabrication parameters with insight on the *in vitro* biological effectiveness. *Drug Des Dev Ther.* 2022;16:3847-64. doi: [10.2147/DDDT.S383051](https://doi.org/10.2147/DDDT.S383051), PMID [36388080](https://pubmed.ncbi.nlm.nih.gov/36388080/).
41. Uddin R, Sansare V. Design, fabrication and evaluation of ketorolac tromethamine loaded microsphere based colon targeted tablet. *IJAPB.* 2020;6(2):9-13. doi: [10.38111/ijapb.20200602002](https://doi.org/10.38111/ijapb.20200602002).
42. Patel V, Mehta P, Bhatt M. Effect of polymer concentration and drug: polymer ratio on the characterization of NSs. *Asian J Pharm.* 2020;14(2):84-92.
43. Zhang Z, Li X, Wang Z. NSs as drug delivery systems: a comprehensive review. *J Drug Deliv Sci Technol.* 2020;55:101375.
44. Mahalakshmi V, Balakrishnan N, Parthasarathy V. Recent advancement of NSs in pharmaceutical formulation for drug delivery systems. *J Appl Pharm Sci.* 2023;13(8):84-100.

45. Patel H, Desai R, Sharma M. Morphological characterization of drug-loaded NSs using FESEM. *Int J Pharm Sci Nanotechnol.* 2023;16(2):234-41.
46. Hussein HH, Kassab HJ. Comparison between ethylcellulose and polymethacrylate topical nanosponges loaded with butenafine hydrochloride. *IJDDT.* 2023;13(1):23-8. doi: [10.25258/ijddt.13.1.04](https://doi.org/10.25258/ijddt.13.1.04).
47. Gabera DA, Radwanb MA, Alzughhaibic DA, Alailc JA, Aljumahc RS, Aloqlac RM. Formulation and evaluation of piroxicam NS. *Drug Deliv.* 2023;30:1-10. doi: [10.1080/10717544.2022.2144541](https://doi.org/10.1080/10717544.2022.2144541), PMID 36453025.
48. Lukic M, Pantelic I, Savic SD. Towards optimal pH of the skin and topical formulations: from the current state of the art to tailored products. *Cosmetics.* 2021;8(3):69. doi: [10.3390/cosmetics8030069](https://doi.org/10.3390/cosmetics8030069).
49. Rao R, Kumar L, Singh G. Rheological characterization and stability analysis of novel hydrogel formulations. *Int J Pharm Sci Res.* 2023;14(5):1109-18.
50. Perez Robles S, Carotenuto C, Minale M. HPMC hydrogel formation mechanisms unveiled by the evaluation of the activation energy. *Polymers.* 2022;14(3):635. doi: [10.3390/polym14030635](https://doi.org/10.3390/polym14030635), PMID 35160624.
51. Salih OS, Al-Akkam EJ. Preparation, in vitro, and ex-vivo evaluation of ondansetron loaded invasomes for transdermal delivery. *IJPS.* 2023;32(3):71-84. doi: [10.31351/vol32iss3pp71-84](https://doi.org/10.31351/vol32iss3pp71-84).
52. Gupta R, Sharma M, Yadav A. Comparative study of nanoparticle synthesis methods: emulsion solvent diffusion vs. ultrasound-assisted synthesis. *Mater Sci Eng C Mater Biol Appl.* 2022;130:112424.
53. Liu Y, Wang J, Zhang X. Optimization of NSs for drug delivery using emulsion solvent diffusion technique. *J Drug Deliv Sci Technol.* 2024;78:103932.
54. Ahmed A, Ali S, Khan H. Synthesis of NS formulations using emulsion solvent diffusion: evaluation and characterization. *Int J Pharm.* 2023;618:121583.
55. Ostrozka Cieslik A, Wilczynski S, Dolińska B. Hydrogel formulations for topical insulin application: preparation, characterization and *in vitro* permeation across the Strat-M® membrane. *Polymers.* 2023;15(17):3639. doi: [10.3390/polym15173639](https://doi.org/10.3390/polym15173639), PMID 37688265.
56. Patel S, Sharma M, Singh G. Enhanced drug release from NS-based hydrogel formulations: an *in vitro* study. *Int J Pharm Sci Res.* 2023;14(8):1250-60.
57. Farsana P, Sivakumar R, Haribabu Y. Hydrogel based nanosponges drug delivery for topical applications-a updated review. *Res J Pharm Technol.* 2021;14(1):527-30. doi: [10.5958/0974-360X.2021.00096.2](https://doi.org/10.5958/0974-360X.2021.00096.2).
58. Mehta A, Sing A, Mehta S. Increased screen time during the pandemic: lessons learnt. *Int J Health Sci Res.* 2023;13(1):1-7. doi: [10.52403/ijhsr.20230101](https://doi.org/10.52403/ijhsr.20230101).
59. Tiwari K, Bhattacharya S. The ascension of NSs as a drug delivery carrier: preparation, characterization, and applications. *J Mater Sci Mater Med.* 2022;33(28).
60. Sivadasan D, Venkatesan K, Mohamed JM, Alqahtani S, Asiri YI, Faisal MM. Application of ³²factorial design for loratadine-loaded nanosponge in topical gel formulation: comprehensive *in vitro* and ex vivo evaluations. *Sci Rep.* 2024;14(1):6361. doi: [10.1038/s41598-024-55953-2](https://doi.org/10.1038/s41598-024-55953-2), PMID 38493177.